Photochemical Modification of Cross-Linked Poly(dimethylsiloxane) by Irradiation at 172 nm

Vera-Maria Graubner, Rainer Jordan, and Oskar Nuyken*

Technische Universität München, Lehrstuhl für Makromolekulare Stoffe, Lichtenbergstrasse 4, 85747 Garching, Germany

Bernhard Schnyder, Thomas Lippert,* Rüdiger Kötz, and Alexander Wokaun

Paul Scherrer Institut, General Energy Department, 5232 Villigen, Switzerland

Received February 5, 2004; Revised Manuscript Received June 7, 2004

ABSTRACT: Cross-linked poly(dimethylsiloxane) (PDMS) was irradiated with a Xe_2*-excimer lamp (172 nm) under ambient conditions. The irradiation in combination with the formed ozone results in an oxidation of PDMS to SiO_2 at the polymer−air interface. The surface properties of the irradiated surfaces were studied by means of contact angle measurements, infrared spectroscopy, and X-ray photoelectron spectroscopy. The photochemical conversion of surface methylsilane groups to silanol groups is responsible for the large increase in surface free energy. Subsequent degradation of the polymer and formation of SiO_x was monitored by infrared spectroscopy. As determined by X-ray photoelectron spectroscopy, the binding energy shifts reach values corresponding to SiO_2. The atomic ratio concentration O:Si changes from about 1:1 (PDMS) to about 2:1 (SiO_2). On the basis of the XPS and IR results, the photochemical reaction pathway from PDMS to silicon oxide via surface silanol groups is discussed. The strict linearity of the contact angle versus irradiation time and the clear dependence from irradiation intensity allows the tuning of the chemical surface functionalities.

Downloaded by BBWS CONSORTIA GERMANY on August 3, 2009
Published on July 17, 2004 on http://pubs.acs.org | doi: 10.1021/ma049747q

Introduction

Poly(dimethylsiloxane)s (PDMS) are widely used as coatings in a variety of fields including biomedical applications such as membrane technology, microlithography, optics, and dielectrics.[1,2] Cross-linked poly(siloxane)s possess unique mechanical, nearly ideal elastomer and optical properties, low weight, high durability, high gas permeability, and excellent water repellency.[3,4] The modification of the hydrophobic PDMS to hydrophilic SiO_x opens an additional wide range of applications, that is, in microelectronics[5−7] and coating technology for medical devices.[8−10] Its scratch resistance, gas barrier properties, and high thermal stability have encouraged the synthesis of SiO_x thin films from PDMS by different routes. However, most of the described methods suffer from specific preparation methods, restrictive atmospheric conditions, high temperatures, and/or rather long reaction times. Seyferth[11] reported on the pyrolytic degradation of PDMS, which results in high-quality silicon oxide films only at temperatures above 800 °C. Koberstein and Mirley[12] described a facile process for the preparation of silicon oxide. They transformed Langmuir−Blodgett films prepared from diacid-terminated PDMS to ultrathin SiO_x films by irradiation with a low-pressure mercury-quartz lamp (185−254 nm) at room temperature in air. A 14 Å thick film of silicon oxide with 10% residual hydrocarbon content was obtained. Hillborg et al.[13] reported on the processing of PDMS with radio frequency or microwave oxygen plasma. The treatment was performed at a pressure of 3 mbar of ultrapure oxygen and led to the formation of a smooth (rms < 10 nm) oxidized surface layer with a thickness of 130−160 nm. The resulting oxide layer contained a mixture of the original polymer and silicon bonded to three or four oxygen atoms (SiO_x). As an alternative, the pulsed laser deposition (PLD) technique was employed to deposit SiO_2 thin films by ablation of poly(dimethylsiloxane) with a 193 nm ArF excimer laser at an oxygen gas pressure of 10^{-1} to 10^{-4} mbar.[14] In terms of a future technological application, a surface modification of the hydrophobic PDMS material to a reactive and hydrophilic SiO_x layer under ambient conditions with short reaction times is desirable. For this purpose, excimer lamps, which provide high-intensity, high-efficiency, and narrow-band radiation, may be appropriate. Recent applications of excimer lamps include photodeposition of large area or patterned thin metal films,[15,16] photoassisted low-temperature oxidation of Si,[17] SiGe,[18] and Ge,[19] UV curing,[20] polymer etching and microstructuring of polymer surfaces,[21,22] and recently even for the nitriding of polyolefin surfaces.[23] Vacuum ultraviolet sources, such as cold plasmas[24−26] and VUV resonance lamps,[27,28] have also been applied to study the transformation and degradation of organic polymers,[24−27] or to improve the microwear resistance.[28] The VUV irradiation of cold plasmas has also been used to simulate certain conditions in outer space to test the long-term stability of materials under these conditions.[29,30]

Here, we report on an improved and straightforward photochemical modification of PDMS surface with a Xe_2*-excimer lamp at 172 nm irradiation. The photochemical-modified PDMS surfaces were studied by contact angle measurements, X-ray photoelectron spectroscopy (XPS), and attenuated total reflection (ATR) Fourier transform infrared (FTIR) spectroscopy.

* To whom correspondence should be addressed. (O.N.) Telephone: +49 (0)89 289 13570. Fax: +49 (0)89 289 13562. E-mail: oskar.nuyken@ch.tum.de. (T.L.) Telephone: +41 (0)56 310 4076. Fax: +41 (0)56 310 2199. E-mail: thomas.lippert@psi.ch.

10.1021/ma049747q CCC: $27.50 © 2004 American Chemical Society
Published on Web 07/17/2004

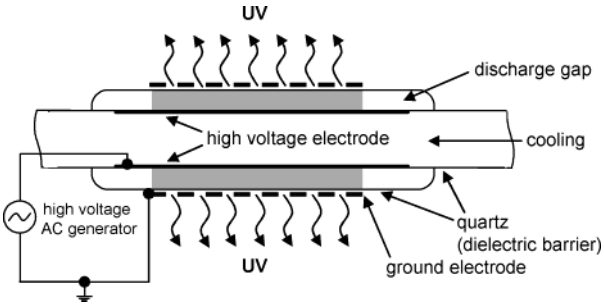

Figure 1. Sketch of the water-cooled Xe_2*-excimer lamp (λ = 172 nm).

Experimental Section

Materials. Films of cross-linked PDMS, supplied by AGFA, were used as received. They were prepared by bar coating of a 12 wt % solution of vinyl-functionalized poly(dimethylsiloxane), poly(methylhydrosiloxane) as a cross-linker, and a Karstedt platinum catalyst in isooctane on poly(ethylene terephthalate) plates. After evaporation of the solvent, the films were cured for 5 min at 100 °C, resulting in an average film thickness of about 8 μm.

UV Source. Exposure to vacuum ultraviolet (VUV) light was performed with a water-cooled VUV excimer lamp of 3 cm in diameter and approximately 30 cm length (see Figure 1), mounted in a homemade irradiation chamber. The discharge was initiated in an annular gap between two coaxial quartz tubes containing xenon at 750 mbar emitting at a wavelength of 172 nm (fwhm 20 ± 7.5 nm). Tubes of Suprasil 1 quartz were chosen as dielectric barriers because of its dielectric properties and its superior UV transmission.[31]

The excimer VUV source was operated at frequencies of 225−280 kHz and a voltage amplitude of 10 kV. The fluence was determined in air with a XUV detector (Gigahertz-Optik, Germany) equipped with a far ultraviolet photodiode in combination with a 172 nm standard band-pass filter (fwhm 20 ± 7.5 nm, Acton Research). The PDMS surfaces were irradiated at ambient conditions in air with intensities of 10.4 and 16.6 mW/cm^2 at a distance of 5 mm to the UV source.

Contact Angle Measurements. The wettability of the VUV/ozone-treated samples was studied using a contact angle goniometer G 2 from Krüss GmbH, Germany. Each given contact angle value (Table 1 and Figure 2) is the average of measurements from at least five different spots on the respective sample surface. We employed the sessile drop technique (drop volume 4 μL) with bidistilled water and diiodomethane (Fluka).

X-ray Photoelectron Spectroscopy (XPS). XPS analyses of samples irradiated for different time periods were performed on an ESCALAB 220i XL instrument (Thermo VG Scientific). The photoelectron spectrometer was equipped with a magnesium X-ray source ($h\nu$ = 1253.6 eV). The source was operated at 100 W to minimize beam damage of the sample. Measured binding energies were referred to the C 1s signal at 284.6 eV. The spectra were recorded in the constant analyzer energy mode with analyzer pass energies of 50 eV for the survey spectra and 20 eV for the high-resolution detail spectra.

Infrared Spectroscopy. Attenuated total reflection Fourier transform infrared (ATR-FTIR) spectra were recorded with a Perkin-Elmer 2000 FTIR spectrometer equipped with a ATR accessory from Specac. The spectrometer was equipped with a nitrogen-cooled MCT detector. Spectra (sum of 128 scans) were recorded in the range of 4000−650 cm^{-1} with a spectral resolution of 4 cm^{-1}. A ZnSe crystal with 45° beam incidence allowing six reflections at the interface was used. The spectrum of a freshly cleaned crystal was used as the background.

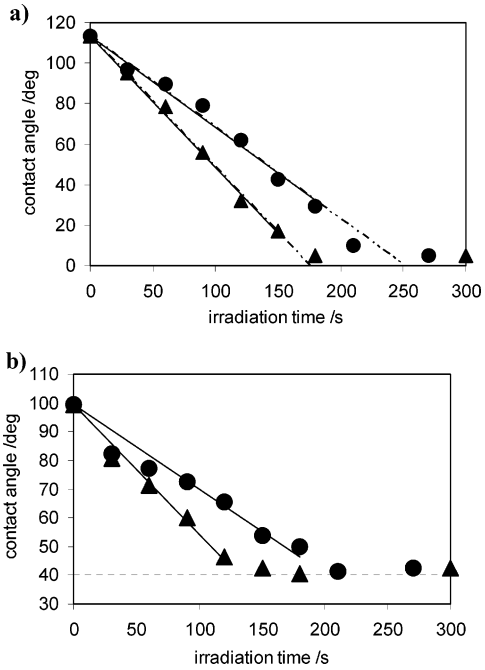

Figure 2. (a) Static water contact angle on PDMS surfaces versus irradiation time for two different intensities (● 10.4 mW/cm^2; ▲ 16.6 mW/cm^2). The solid lines are calculated by linear regression. (b) Static diiodomethane contact angle on PDMS surfaces versus irradiation time for various intensities. The solid lines are calculated by linear regression. The dotted line represents the lower limit (40°) of the static diiodomethane contact angle. The error of each given data point is within 4°.

Table 1. Contact Angle Data and Corresponding Surface Free Energy (γ) with Polar (γ_{pol}) and Disperse (γ_{disp}) Components (Owens−Wendt−Rabel−Kaelble Method) and Corresponding Surface %OH (Cassie and Israelachvili & Gee) of PDMS Surfaces Exposed to 172 nm Irradiation in Air (16.6 and 10.4 mW/cm^2)

	c.a./deg		γ/	γ_{pol}/	γ_{disp}/	surface %OH	
t/min	H_2O	CH_2I_2	(mN/m)	(mN/m)	(mN/m)	I&G	Cassie
			16.6 mW/cm^2				
0.0	113.4	99.5	8.9	1.4	7.5	0.0	0.0
0.5	95.0	80.9	17.6	4.8	12.8	12.9	22.2
1.0	78.8	71.3	26.5	13.3	13.2	29.2	42.3
1.5	55.8	59.9	44.7	32.3	12.5	57.1	68.7
2.0	31.8	46.2	63.8	50.0	13.8	84.1	89.3
2.5	16.9	42.5	72.5	59.2	13.3	95.3	96.9
3.0	5.0	40.4	75.7	62.3	13.4	99.6	99.7
5.0	5.0	42.6	76.3	63.9	12.4	99.6	99.7
60.0	0.0	39.6	75.9	62.2	13.7	100	100
			10.4 mW/cm^2				
0.0	113.4	99.5	8.9	1.4	7.5	0.0	0.0
0.5	96.7	82.3	16.7	4.3	12.5	11.5	20.1
1.0	89.7	77.1	20.3	6.9	13.4	17.8	28.8
1.5	79.0	72.4	26.2	13.7	12.5	29.0	42.1
2.0	61.9	65.5	39.7	28.6	11.1	49.5	62.1
2.5	42.8	53.9	56.0	43.8	12.2	72.7	80.9
3.0	29.4	49.9	66.7	55.2	11.5	86.3	90.8
3.5	9.8	41.2	74.9	61.6	13.3	98.4	99.0
4.5	5.0	42.6	76.3	63.9	12.4	99.6	99.7

Results and Discussion

Contact Angle Measurements. The modification of the PDMS surface by reactive irradiation with a Xe_2*-excimer lamp was studied by wetting experiments. Figure 2 shows the static contact angles of the PDMS substrates for deionized water (a) and diiodomethane (b) as a function of irradiation time with irradiation times from 10 to 300 s at fluences of 10.4 and 16.6 mW/cm^2.

Downloaded by BBWS CONSORTIA GERMANY on August 3, 2009
Published on July 17, 2004 on http://pubs.acs.org | doi: 10.1021/ma049747q

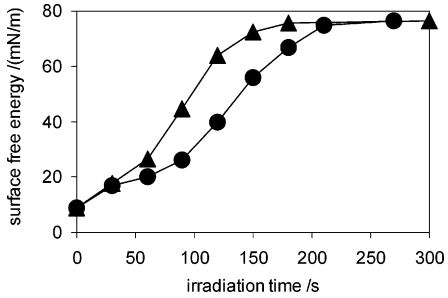

Figure 3. Surface free energies of PDMS surfaces versus irradiation time for various intensities. For calculation, the Owens−Wendt−Rabel−Kaelble method was applied to the linear regression plots of the raw contact angle data (Figure 2) (● 10.4 mW/cm^2; ▲ 16.6 mW/cm^2).

As is apparent from Figure 2, upon proceeding irradiation, the contact angles undergo a strictly linear decrease. The water contact angle of the native PDMS surface is 110° (hydrophobic) and decreases to <5° (spreading), whereas the diiodomethane contact angle decreases from 90° to 40° within minutes of irradiation. The decrease is even more rapid but still linear when higher fluences were applied. At longer irradiation times (e.g., 30 min), no further changes of the contact angles could be detected.

The contact angle of a liquid on a surface is directly correlated to the surface free energy. The surface free energy is assumed to consist of two additive parts, a polar component, which accounts for the dipole−dipole and H-bonding interactions, and a dispersive component, which accounts for London type (van der Waals) forces. One approach of describing the wettability of the heterogeneous surface is to analyze the dispersion and polar components of the surface free energy with the Owens−Wendt−Rabel−Kaelble[32−35] method. The results of these calculations based on the contact angle data are given in Figure 3. The contact angle values with the calculated surface free energies are summarized in Table 1.

We observed a significant increase in the surface free energy in the form of an S-shaped curve. The increase is even more rapid at higher fluences. Regarding the particular components of the surface free energy, this remarkable change can be ascribed to significant changes in the polar interactions (Figure 4a). As outlined below, these polar interactions are originating from surface silanol groups generated by the VUV treatment in the presence of O_2.

The dispersion component of the surface free energy does not change significantly (Figure 4b). This can be expected because dispersion forces are very weak forces of attraction between molecules and are proportional to the number of electrons present in the molecule. Regarding the repeating unit of PDMS ($-Si(CH_3)_2O-$), the number of valence electrons (24 e$^-$) does not change by substitution of methyl groups by hydroxyl groups resulting in $-Si(CH_3,OH)O-$ and $-Si(OH)_2O-$. Thus, there is no significant effect detectable in the dispersive component of the surface free energy. The initial increase of about 60% is most probably due to the removal of low molecular weight impurities from the interface.[36,37]

Another interpretation of the wetting behavior of heterogeneous surfaces is the implementation of the phenomenological Cassie equation[38−42] and the Israelachvili & Gee equation.[43] The Cassie equation (eqs 1 and 2) conceptually describes the averaging adhesion energies between the liquid and the surface with respect to fractional coverage of the two surface functionalities:

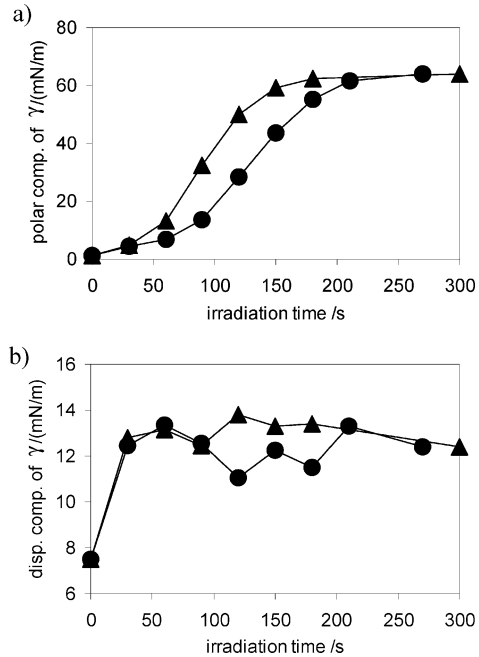

Figure 4. (a) Polar component of the surface free energy (γ) of PDMS surfaces versus irradiation time for various intensities. (b) Dispersive component of the surface free energy (γ) of PDMS surfaces versus irradiation time for various intensities. For calculation, the Owens−Wendt−Rabel−Kaelble method was applied to the linear regression plots of the raw contact angle data (Figure 2) (● 10.4 mW/cm^2; ▲ 16.6 mW/cm^2).

$$W = f_1 W_1 + f_2 W_2 \quad (1)$$

$$\cos\theta = f_1 \cos\theta_1 + f_2 \cos\theta_2 \quad (2)$$

where W is the total adhesion energy, and W_1 and W_2 are the adhesion energies of the homogeneous surfaces 1 and 2, respectively. The contact angle θ of a liquid on a heterogeneous surface is composed of a fraction f_1 of chemical groups type 1 (methyl groups) and f_2 of groups type 2 (hydroxyl groups) with $f_1 + f_2 = 1$, where θ_1 and θ_2 are the contact angles on the pure homogeneous surfaces.

In deriving the Israelachvili & Gee equation (eq 3), it is argued that the contact angle of the surface, with heterogeneities on the molecular scale, is determined by the polarization of the surface and of the probing liquid. They suggested that the relevant properties to be averaged, with respect to surface fractional coverage, are the surface polarizabilities, dipole moments, or charges, rather than the adhesion energies.

$$(1 + \cos\theta)^2 = f_1(1 + \cos\theta_1)^2 + f_2(1 + \cos\theta_2)^2 \quad (3)$$

This equation replaces the Cassie equation whenever the sizes of the chemically heterogeneities approach molecular or atomic dimensions. It should be noted, however, that this approach does not take into account the interactions among surface functional groups.

Figure 5a shows the variation of the surface OH concentration as calculated by the Cassie equation and the Israelachvili & Gee equation in air as a function of the irradiation time. It was found that within 180 s of irradiation at 16.6 mW/cm^2 and within 240 s of irradia-

Downloaded by BBWS CONSORTIA GERMANY on August 3, 2009
Published on July 17, 2004 on http://pubs.acs.org | doi: 10.1021/ma049747q

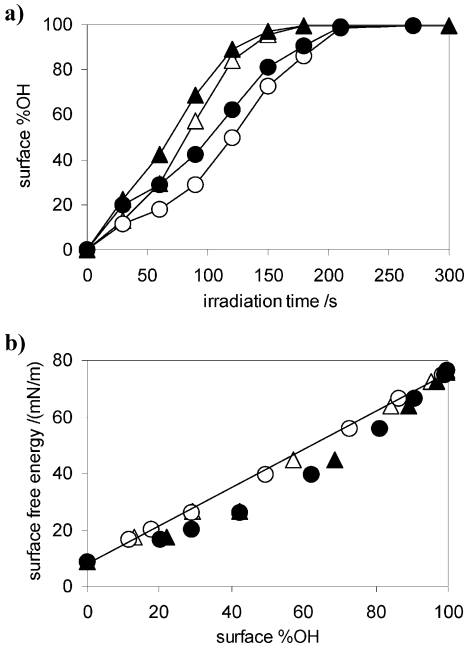

Figure 5. (a) Surface OH concentration on PDMS surfaces versus irradiation time for various intensities as calculated by the Cassie (●, ▲) and the Israelachvili & Gee (○, △) equation (●/○ 10.4 mW/cm^2; ▲/△ 16.6 mW/cm^2). (b) Surface free energy of irradiated PDMS surfaces versus surface OH concentration on irradiated PDMS surfaces as calculated by the Cassie (●, ▲) and the Israelachvili & Gee (○, △) equation (●/○ 10.4 mW/cm^2; ▲/△ 16.6 mW/cm^2).

tion at 10.4 mW/cm^2, the surface OH concentration reaches 100% (up to this amount of OH groups changes in the contact angle can be detected). At the same irradiation times, the water contact angles reach their minima (<5°) and the surface free energies as calculated by the Owens–Wendt–Rabel–Kaelble method reach their maxima (Figures 2 and 3). This is equal to the complete spreading condition of a water droplet on the surface.

Combining the Israelachvili & Gee approach for heterogeneous surfaces with the surface free energy calculations by the Owens–Wendt–Rabel–Kaelble method, a linear correlation between the surface free energy and the OH concentration on the surface is obtained (Figure 5b). The surface free energy is directly dependent on the OH concentration on the surface and reaches its maximum when the OH concentration is maximal. By applying the Cassie equation, the surface free energy does not follow a linear shape. The calculated OH concentrations are generally higher than those calculated by the Israelachvili & Gee equation, except at zero and maximum OH concentration on the surface. This fact is due to the different approaches of Israelachvili & Gee and Cassie by describing the wettability of heterogeneous surfaces. The included surface polarizabilities, dipole moments, and dipole charges by Israelachvili & Gee result in a higher surface free energy for a given surface OH concentration by simply considering the adhesion energy of the surface and the droplet.

In summary, after exposure to 172 nm irradiation in air, the contact angles of water and diiodomethane followed a remarkable and linear decrease due to the formation of surface silanol groups. The OH concentration on the surface is linearly correlated with the surface free energy when combining the Israelachvili & Gee approach with the Owens–Wendt–Rabel–Kaelble method.

Table 2. Atomic Concentration (at. %) Determined by XPS of Native PDMS and PDMS Exposed to 172 nm Irradiation in Air (16.6 mW/cm^2, 5 mm, 2 and 40 min)[a]

	C (at. %)	O (at. %)	Si (at. %)
PDMS (theor.)	50.0	25.0	25.0
PDMS (exp.)	47.1	25.1	27.7
2 min expos.	21.1	50.3	28.6
40 min expos.	3.2	64.3	32.5

[a] The experimental data are compared to the theoretical values for PDMS without considering the hydrogen, which cannot be detected by XPS.

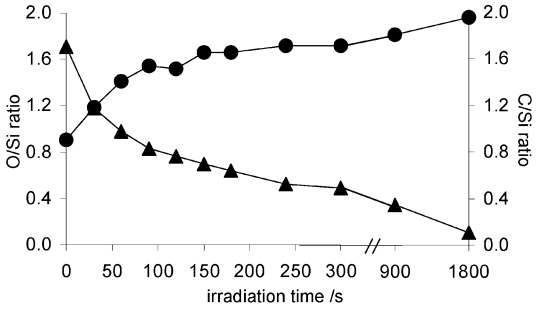

Figure 6. Changes of O/Si (●) and C/Si (▲) atomic concentration ratio of PDMS films exposed to 172 nm (16.6 mW/cm^2) versus irradiation time as determined by XPS.

It is noteworthy to mention that surface-oxidized PDMS commonly displays a surface reconstruction process upon storage over longer times. This is expressed by an increase of the water contact angle values and change in the chemical surface composition. This can be accounted for by a migration of bulk PDMS to the new SiO_2 surface to reduce the free surface energy of the substrate. We also observed this phenomenon and found that for PDMS samples irradiated for less than 2 min a complete recovery (in terms of the water contact angle) occurred within ~24–30 h. Longer irradiation times (e.g., 2 and 2.5 min) not only reduce the speed of the surface reconstruction, but also the final static water contact angle values after 125 h of storage time were significantly smaller (typically between 35° and 45°). At higher storage temperatures (e.g., 50 °C), the reconstruction occurs faster, but final values were similar. In summary, we can state that the surface recovery is dependent upon irradiation time and intensity (thickness of the created SiO_2 surface layer) and upon the storage temperature (faster migration of PDMS).

X-ray Photoelectron Spectroscopy (XPS).[44] XPS was applied to correlate the changes of the contact angles on the PDMS surfaces with changes in surface chemistry, that is, the generation of surface silanol groups. The XPS measurements indicate large changes in the chemical composition of the irradiated PDMS surfaces. The XPS C 1s signal decreases drastically with increasing UV-irradiation time. After 2 min of exposure at 16.6 mW/cm^2, the carbon content decreases from 47 at. %, which is close to the theoretical value of 50 at. % (see Table 2), to 21 at. %. After 40 min, a final value of 3 at. % is reached. The decreasing amount of carbon atoms can be confirmed by plotting the C/Si ratio versus irradiation time (Figure 6), because the amount of Si atoms stays constant during irradiation. It is also necessary to consider that a part of the remaining carbon on the sample surface is due to adventitious carbon, detectable on any XPS sample exposed to air prior to the measurements.

Downloaded by BBWS CONSORTIA GERMANY on August 3, 2009
Published on July 17, 2004 on http://pubs.acs.org | doi: 10.1021/ma049747q

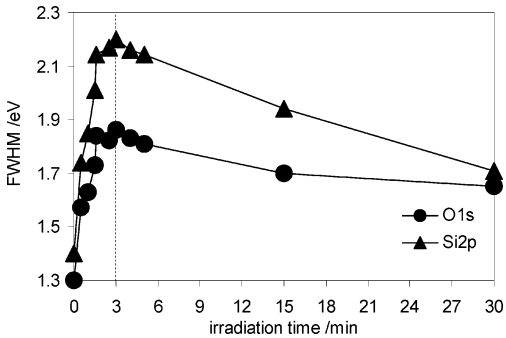

Figure 7. Full width at half-maximum (fwhm) of the O 1s, Si 2p, and C 1s peaks of PDMS films exposed to 172 nm (16.6 mW/cm^2) versus irradiation time.

The atomic concentration ratio of O/Si starts at about 1, which corresponds to the expected value of PDMS, and reaches values close to 2 with increasing irradiation time, which is consistent with the composition of SiO_2 (Figure 6). The creation of SiO_2 is also confirmed by the shifts of the peak positions of the Si 2p and the O 1s signals. The Si 2p binding energy for untreated PDMS of 102.1 eV shifts to 103.4 eV after 40 min of exposure. This peak position corresponds nicely with literature values of 103.3−103.7 eV for SiO_2.[45] For the O 1s level, the corresponding peak shifts from 532.3 eV for untreated PDMS to 533.1 eV after an irradiation time of 40 min. Again, the measured value corresponds quite well with the published data for SiO_2.[45]

Another change in the XPS peak can be observed for irradiation times of <3 min. The full width at half-maximum (fwhm) values of the Si 2p and O 1s increase rapidly for the first 3 min, followed by a slow decrease over the next 30 min (Figure 7). This may correspond to different chemical environments of the Si and the O atoms that can appear with substitution of methyl groups by hydroxyl groups and oxygen, respectively.

Infrared Spectroscopy. IR spectroscopy is an important method for the characterization of polymer conformation,[46] orientation,[47] and solvent effects[48] as well as dynamic processes by time-resolved[49,50] and two-dimensional techniques[51,52] and in situ monitoring of chemical and structural changes.[53,54] Infrared spectroscopy was applied to verify the assumed formation of surface silanol groups and SiO_2 with exposure to VUV in the presence of O_2. Because hydrogen is not detectable by XPS, an exact formulation of the change in the surface chemistry is not possible.

The chemical changes of the PDMS surfaces exposed to VUV in the presence of O_2 were studied by ATR-FTIR spectroscopy. The reference spectrum of the cross-linked PDMS (Figure 8a) is in accordance with previous published data.[55] The bands originating from the symmetric and asymmetric stretching vibrations of the methyl groups ($\nu_{s,as}(CH_3)$) are centered at 2963 and 2906 cm^{-1}, respectively. The corresponding deformation vibrations ($\delta(CH_3)$) modes are located at 1446, 1412, and 1258 cm^{-1}. The asymmetric stretching vibrations of the Si−O−Si group (ν_{as}(SiOSi)) appear between 930 and 1200 cm^{-1}, the methyl rocking ($\rho_r(CH_3)$) and Si−C stretching vibrations (ν(SiC)) are centered around 800 cm^{-1}, and the Si−O bending vibrations (δ(SiO)) are located at about 725 cm^{-1}. The measurement series plotted in Figure 8 are representative of irradiation experiments at intensities at 10.4 and 16.6 mW/cm^2. A quantitative analysis of the spectra was not possible, due to the experimental procedure (e.g., variation in optical contact between crystal and sample, background drift, etc.). Each series of measurements was made with one individual PDMS sample.

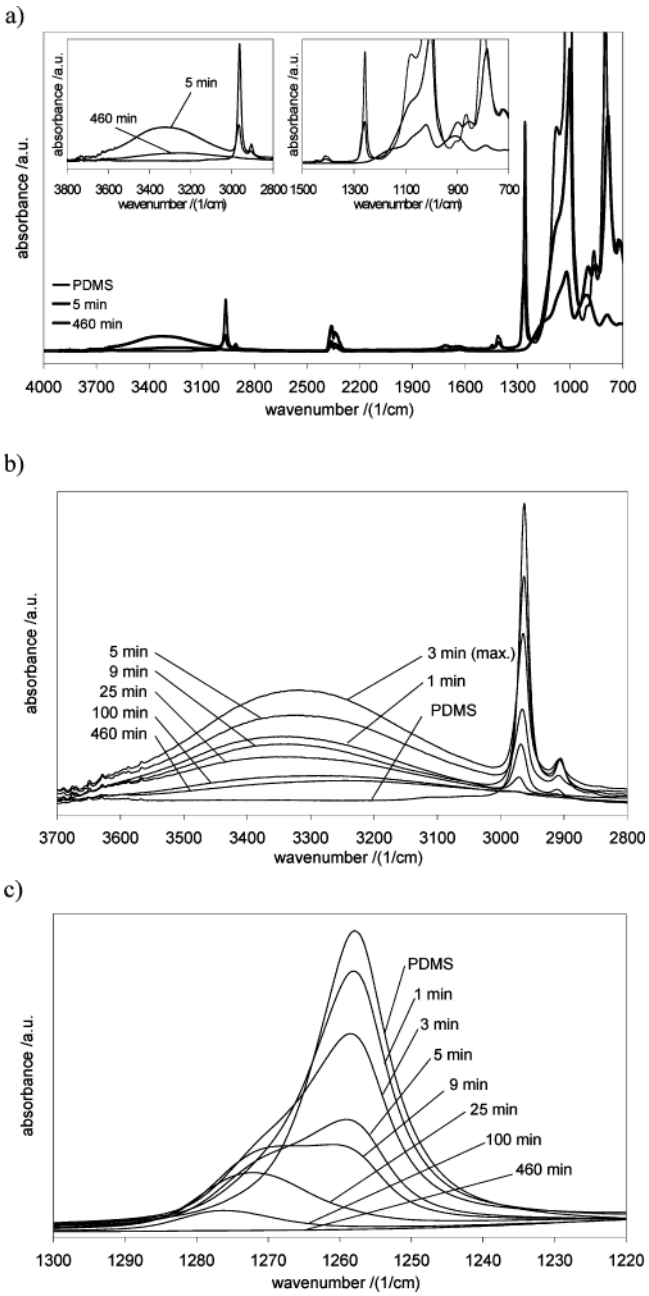

Figure 8. (a) ATR FT-IR spectra of PDMS and irradiated PDMS surfaces (5 and 460 min at 16.6 mW/cm^2). (b) Changes in the OH (around 3300 cm^{-1}) and symmetric and asymmetric ν(C−H) bands (2960 and 2905 cm^{-1}) of PDMS films exposed to 172 nm irradiation (16.6 mW/cm^2). (c) Changes in the δ(C−H) band at 1258 cm^{-1} of PDMS films exposed to 172 nm irradiation (16.6 mW/cm^2).

An overall decrease of PDMS absorption bands was observed, indicating a steady degradation of the siloxane polymer. In addition, initially increasing absorption bands could be detected around 3300, 1275, 1150, and 900 cm^{-1}.

Figure 8b shows the VUV/ozone-induced increase in a broad absorption band centered at 3300 cm^{-1}, indicating the formation of hydroxyl groups on the surface.[56] After 3 min of exposure (16.6 mW/cm^2), the Si−OH absorption band (3300 cm^{-1}) reaches its maximum intensity. It is decreasing for longer irradiation times.

Downloaded by BBWS CONSORTIA GERMANY on August 3, 2009
Published on July 17, 2004 on http://pubs.acs.org | doi: 10.1021/ma049747q

Scheme 1

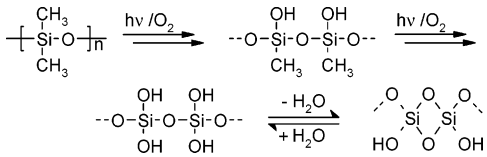

Scheme 2

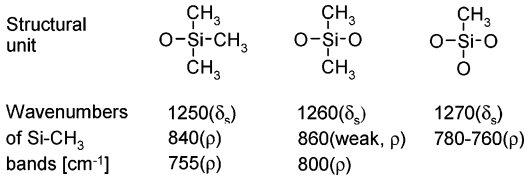

This behavior is in excellent correlation with the observations of the contact angle (Figure 2) and the XPS experiments (Figure 7).[44] At the same irradiation time at which the peak area of the OH absorption band in the IR spectra reaches its maximum, also the full width at half-maximum (fwhm) values of the O 1s and the Si 2p signals reach their maxima, and the surfaces became completely wettable by water. All of this can be ascribed to the formation of Si−O−Si bonds by the elimination of water (Scheme 1). The concomitant increasing and then decreasing absorption band at about 900 cm^{-1} corresponding to the ν(SiO) of the silanol group[57] corroborates this explanation.

In Figure 8c, the decrease of the very strong sharp band at 1258 cm^{-1} originating from $\delta_s(CH_3)$ can be observed. At the same time, $\rho_r(CH_3)$ and ν(Si−C) centered at about 797 cm^{-1} are decreasing. This is accompanied by a shift toward lower wavenumbers (774 cm^{-1}, Figure 8). The infrared band at 1258 cm^{-1} belongs to the structural unit composed of silicon bonded to two oxygen and two methyl groups (Scheme 2).[58] During irradiation in the presence of O_2/O_3, the methyl groups are successively substituted by hydroxyl groups. This is proven by the decreasing $\delta_s(CH_3)$ band at 1258 cm^{-1} and its simultaneous increase between 1270 and 1280 cm^{-1}. The latter represents a structural unit composed of Si bonded to three oxygen atoms and one methyl group.[58] With further irradiation, the second methyl group in the structural unit is substituted by a hydroxyl group, and the $\delta_s(CH_3)$ band between 1270 and 1280 cm^{-1} disappears. The polymer is then almost completely decomposed and transformed to inorganic silicon oxide.

The degradation process of the polymer can also be followed by the decrease and final disappearance of absorption bands assigned to $\nu_s(CH_3)$ (2960 cm^{-1}), $\nu_{as}(CH_3)$ (2905 cm^{-1}), and $\delta_s(CH_3)$ (around 1410 cm^{-1}) as shown in Figure 6. A slight shift of $\nu_s(CH_3)$ and $\nu_{as}(CH_3)$ toward higher wavenumbers during continuous irradiation is detected. This is most probably due to the subsequent replacement of methyl groups by oxygen units at the silicon due to the UV/ozone treatment.

Subsequent degradation of the polymer is also indicated by the overall decrease of ν_{as}(SiOSi) and δ(SiO) of the PDMS present between 750 and 1200 cm^{-1}. With increasing irradiation time, ν_{as}(SiOSi) at 1000 cm^{-1} gradually shifts toward higher wavenumbers due to an increasing number of oxygen atoms at the silicon. At the same time, a shoulder appears around 1150 cm^{-1}. Lucovsky et al.[59] and Pai et al.[60] calculated the IR spectrum of SiO_2 and suggested that the broad shoulder around 1150 cm^{-1} belongs to the out-of-phase oxygen motion associated with a $Si(O_4)$ configuration.

Scheme 3

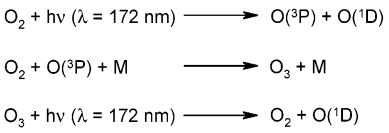

The IR spectrum of the modified PDMS surface after 460 min of exposure to 172 nm irradiation in air (Figure 8) exhibits absorption maxima at 3247 (ν(OH)), intermolecular bonding), 1625 (OH bending vibrations (δ(OH)) of molecular water[61]), 1021 (ν_{as}(SiOSi)) with a shoulder around 1150, 908 (ν(SiO) of Si−OH group[49]), and 790 cm^{-1} (δ(SiO)[61]). Because CH_3 vibrations are no longer detectable, it can be assumed that the PDMS surface was quantitatively decomposed and SiO_x is formed within the information depth of the ATR technique (approximately 0.5−2 μm).

Comparing the changes in chemical composition as detected by XPS and infrared spectroscopy to the wettability behavior at increasing irradiation time, we concluded that the time scale of the maximum change scales with the sampling depths of the applied method. This can be understood by the fact that the goniometry, as a surface-sensitive method, probes only the very top surface layer. For XPS, the information depth is in the range of 5−10 nm. As compared to the infrared spectroscopy experiments, the changes in the chemical composition as detected by XPS occur even faster because the information depth in ATR spectroscopy is between 0.5 and 2 μm.

Mechanism of VUV Oxidation. The mechanisms of the thermal, photothermal, and photochemical oxidation of PDMS to silicon oxide in the presence of oxygen and/or ozone have been discussed in the literature.[62−69] In general, it is suggested that the abstraction of hydrogen is the initial step. The resulting methylene radical reacts with oxygen to give a peroxy radical and rearranges to the silanol group.

The absorption cross section of oxygen at 172 nm irradiation is 6×10^{-19} cm^2.[70] Because the concentration of oxygen in air is about 21%, the intensity of the radiation is reduced to about 1/100 after 0.6 mm. The processes involved in the VUV absorption in oxygen are shown in Scheme 3).[71]

Ozone is then formed in an excited state by a three-body reaction of oxygen atoms with oxygen molecules. The fate of this intermediate is mainly determined by quenching processes. Ozone also photodissociates by absorption of the UV radiation and forming oxygen atoms and molecules in the ground and excited state. Eliasson and Kogelschatz performed model calculations of the ozone formation processes in oxygen by using the 172 nm radiation.[71] As compared to ozone, the excited atomic and molecular species stay below 1 ppm. Thus, ozone is an important reaction partner, but the most important part in the oxidation process plays the radiation itself, because PDMS is almost inert to ozone at room temperature.[72] The importance of the VUV photons was also confirmed by irradiating PDMS in an inert gas atmosphere (N_2). Pronounced changes of the contact angle were detected, although not to the extent that was reached by irradiation in air. The changes of the contact angle are probably due to bond breaking in the PDMS and reaction of the products with air after venting the reaction chamber.

The experiments in air were performed with intensities of 10.4 and 16.6 mW/cm^2, and the temperature on

Downloaded by BBWS CONSORTIA GERMANY on August 3, 2009
Published on July 17, 2004 on http://pubs.acs.org | doi: 10.1021/ma049747q

Scheme 4

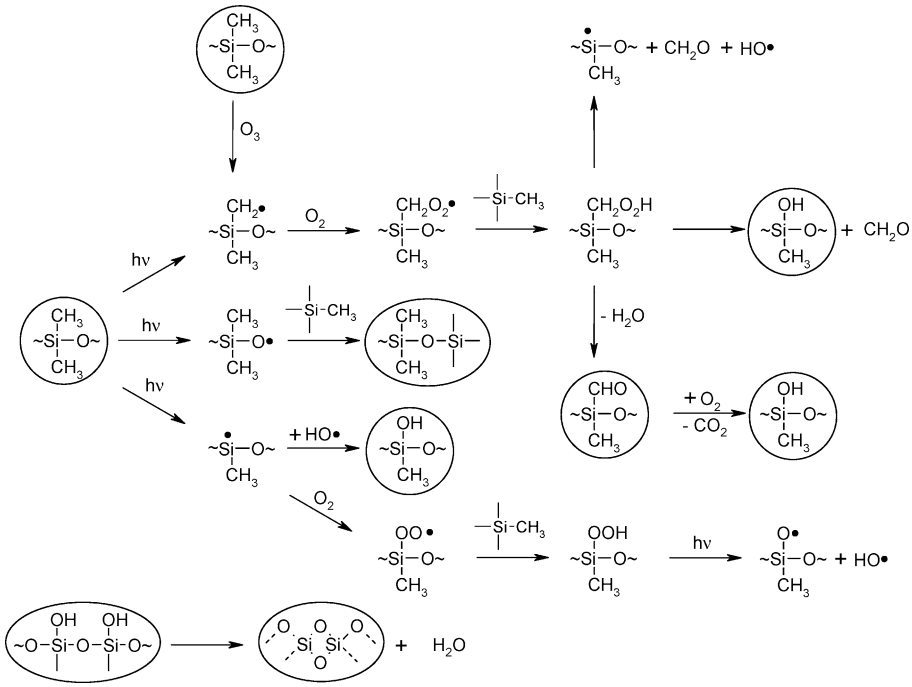

the surface during irradiation reaches approximately 45 °C. The intensity was measured under identical experimental conditions. The absorption coefficient of PDMS at 172 nm irradiation is ~4100 cm^{-1}.[73] Thus, the intensity of the radiation is reduced to about 1/100 after 13.2 μm. As probed by ATR, the oxidation occurs to a layer depth of at least 2 μm (information depth of ATR). The energy of the radiation (7.2 eV) can easily break any bond in the polymer (Si−O, 4.8 eV; Si−C, 3.3 eV; C−H, 4.2 eV) up to several micrometers depth. On one hand, the required oxygen for the oxidation at increasing layer depth is already present in the layer due to the preparation method in air. On the other hand, oxygen can diffuse into deeper layers through polymeric and/or already oxidized material. We assume that the initial step mainly incorporates a bond break either in the main chain (Si−O) or in the side groups of the polymer (Si−C and C−H). Further reactions of the silicon and methylene radicals with oxygen lead to the formation of peroxy radicals, which rearrange to give silanol groups. The oxygen radical can attack a Si−C bond to create a new Si−O−Si bridge. The silicon radical can also react with a hydroxyl radical, which is formed by the absorption of 172 nm irradiation in air, to form a silanol group. A survey of possible reactions involved in the oxidation process of PDMS during irradiation with a Xe_2*-excimer lamp in air is given in Scheme 4. The framed chemical structures were detected by ATR-FTIR measurements.

The formation of stable intermediates including methylene groups could not be verified because corresponding absorption bands were not detected by infrared spectroscopy. However, the formation of carbonyl groups during irradiation (Scheme 4) was verified by a very weak increase and following decrease of a carbonyl absorption band around 1725 cm^{-1} and a band at 1700 cm^{-1} corresponding to hydrogen-bonded carbonyl groups.[69]

Conclusion

Irradiation of PDMS at 172 nm under ambient conditions causes a rapid and controllable surface oxidation of the polymer. The formation of ozone by irradiation in air in combination with the irradiation itself results in the formation of a surface layer consisting of inorganic SiO_2. A rapid and linear increase of the surface free energy due to the formation of surface hydroxyl groups was verified by contact angle measurements, XPS, and IR spectroscopy. The surface silanol groups are formed by abstraction of hydrogen followed by the reaction of the methylene radical with oxygen and further rearrangement. Another possibility of the generation of silanol groups is a bond break in the main chain. Further reaction of the silicon radicals with oxygen or hydroxyl leads to surface silanol groups. Elimination of water from neighboring surface silanol groups results in Si−O−Si bonds on the surface. The observed binding energy shifts of the Si 2p and O 1s peaks correspond quite well to SiO_2. The atomic ratio concentration O:Si changes from about 1:1 (PDMS) to nearly 2:1 (SiO_2). The strict linearity of the contact angle versus irradiation time and the clear dependence from irradiation intensity allow the tuning of the chemical surface functionalities.

Acknowledgment. Financial support from the Bundesministerium für Bildung und Forschung (BMBF) and the Swiss National Science Foundation is gratefully acknowledged. We thank Prof. I. Boyd and Dr. U. Kogelschatz for advice on the operation of the excimer lamp.

References and Notes

(1) Noll, W. *Chemistry and Technology of Silicones*; Academic Press: New York, 1968.

(2) Hillborg, H.; Gedde, U. W. *IEEE Trans. Dielectr. Electr. Insul.* **1999**, *6*, 703.

(3) Gorur, R.; Cherney, E.; Burnham, J. *Outdoor Insulation*; College of Engineering and Applied Science, Arizona State University, 1998.

(4) Campbell, B. Dow Corning Corp. paper, 1996.

(5) Klumpp, A.; Sigmund, H. *Appl. Surf. Sci.* **1989**, *43*, 301−303.

Downloaded by BBWS CONSORTIA GERMANY on August 3, 2009
Published on July 17, 2004 on http://pubs.acs.org | doi: 10.1021/ma049747q

Downloaded by BBWS CONSORTIA GERMANY on August 3, 2009
Published on July 17, 2004 on http://pubs.acs.org | doi: 10.1021/ma049747q

(6) Joubert, O.; Hollinger, G.; Fiori, C.; Devine, R. A. B.; Paniez, P.; Pantel, R. *J. Appl. Phys.* **1991**, *69*, 6647−6651.
(7) Niwano, M.; Kinashi, K.; Saito, K.; Miyamoto, N.; Honma, K. *J. Electrochem. Soc.* **1994**, *141*, 56−61.
(8) Barry, A. *Chem. Technol.* **1983**, *13*, 532−555.
(9) Harvey, N. G.; Tropsha, Y. G.; Burkett, S. L.; Clarke, R. P.; Wong, B. S. Eur. Pat. Appl. 1997, EP 787827; *Chem. Abstr.* 127:210414.
(10) Tropsha, Y. G. Eur. Pat. Appl. 1997, EP 787826; *Chem. Abstr.* 127:210413.
(11) Seyferth, D. *Adv. Chem. Ser.* **1990**, *224*, 565−591.
(12) Mirley, C. L.; Koberstein, J. T. *Langmuir* **1995**, *11*, 1049−1052.
(13) Hillborg, H.; Ankner, J. F.; Gedde, U. W.; Smith, G. D.; Yasuda, H. K.; Wikstrom, K. *Polymer* **2000**, *41*, 6851−6863.
(14) Okoshi, M.; Kuramatsu, M.; Inoue, N. *Appl. Surf. Sci.* **2002**, *197−198*, 772−776.
(15) Esrom, H. *Appl. Surf. Sci.* **2000**, *168*, 1−4.
(16) Boyd, I. W.; Zhang, J. Y.; Bergonzo, P. *Proceedings SPIE-Int. Soc. Opt. Eng.* **1995**, *2403*, 290−301.
(17) Kaliwoh, N.; Zhang, J. Y.; Boyd, I. W. *Appl. Surf. Sci.* **2000**, *168*, 288−291.
(18) Zhang, J.-Y.; Fang, Q.; Kenyon, A. J.; Boyd, I. W. *Appl. Surf. Sci.* **2003**, *208−209*, 364−368.
(19) Craciun, V.; Hutton, B.; Williams, D. E.; Boyd, I. W. *Electron. Lett.* **1998**, *34*, 71−72.
(20) Zhang, J.-Y.; Windall, G.; Boyd, I. W. *Appl. Surf. Sci.* **2002**, *186*, 568−572.
(21) Zhang, J.-Y.; Boyd, I. W.; Esrom, H. *Surf. Interface Anal.* **1996**, *24*, 718−722.
(22) Zhang, J. Y.; Esrom, H.; Kogelschatz, U.; Emig, G. *Appl. Surf. Sci.* **1993**, *69*, 299−304.
(23) Truica-Marasescu, F.; Wertheimer, M. R. *J. Appl. Polym. Sci.* **2004**, *91*, 3886−3898.
(24) Holländer, A.; Klemberg-Saphieha, J. E.; Wertheimer, M. R. *J. Polym. Sci., Part A: Polym. Chem.* **1995**, *33*, 2073.
(25) Holländer, A.; Klemberg-Saphieha, J. E.; Wertheimer, M. R. *J. Polym. Sci., Part A: Polym. Chem.* **1996**, *34*, 1511−1516.
(26) Fozza, A. C.; Roch, J.; Klemberg-Saphieha, J. E.; Kruse, A.; Holländer, A.; Wertheimer, M. R. *Nucl. Instrum. Methods Phys. Res., Sect. B* **1997**, *131*, 205−210.
(27) Skurat, V. E.; Dorofeev, Y. I. *Angew. Makromol. Chem.* **1994**, *216*, 205−224.
(28) Vasilets, V. N.; Nakamura, K.; Uyama, Y.; Ogata, S.; Ikada, Y.; Polymer **1998**, *13*, 2875−2881.
(29) Golub, M. A. *Macromol. Chem., Macromol. Symp.* **1992**, *53*, 379.
(30) Zimcik, M. A.; Wertheimer, M. R.; Balmain, K. G.; Tennyson, R. C. *J. Spacecr. Rockets* **1991**, *652*, 28.
(31) Gellert, B.; Kogelschatz, U. *Appl. Phys. B* **1991**, *52*, 14−21.
(32) Owens, D. K.; Wendt, R. C. *J. Appl. Polym. Sci.* **1969**, *13*, 1741−1747.
(33) Rabel, W. *Farbe Lack* **1971**, *77*, 997−1006.
(34) Kaelble, D. H. *J. Adhes.* **1970**, *2*, 66−88.
(35) Kaelble, D. H. *Physical Chemistry of Adhesion*; Wiley: New York, 1971.
(36) Bautista, M. C.; Rubio, J.; Oteo, J. L. *J. Mater. Sci.* **1995**, *30*, 1595−1600.
(37) Chappell, P. J. C.; Williams, D. R. *J. Colloid Interface Sci.* **1989**, *128*, 450−457.
(38) Wenzel, R. N. *J. Ind. Eng. Chem.* **1936**, *28*, 988−994.
(39) Wenzel, R. N. *J. Phys. Colloid Chem.* **1949**, *53*, 1466−1467.
(40) Cassie, A. B. D.; Baxter, S. *Trans. Faraday Soc.* **1944**, *40*, 546−551.
(41) Baxter, S.; Cassie, A. B. D. *J. Text. Inst.* **1945**, *36*, T67−90.
(42) Cassie, A. B. D. *Discuss. Faraday Soc.* **1948**, *No. 3*, 11−16.
(43) Israelachvili, J. N.; Gee, M. L. *Langmuir* **1989**, *5*, 288−289.
(44) Schnyder, B.; Lippert, T.; Koetz, R.; Wokaun, A.; Graubner, V.-M.; Nuyken, O. *Surf. Sci.* **2003**, *532−535*, 1067−1071.
(45) Moulder, J. F.; Stickle, W. F.; Sobol, P. E.; Bomben, K. D. In *Handbook of X-ray Photoelectron Spectroscopy*; Chastain, J., Ed.; Perkin-Elmer Corp.: Eden Prairie, 1992.
(46) Moyses, S.; Spells, S. J. *Macromolecules* **1999**, *32*, 2684−2689.
(47) Shinomura, M.; Okumoto, H.; Kaito, A.; Ueno, K.; Shen, J.; Ito, K. *Macromolecules* **1998**, *31*, 7483−7487.
(48) Minagawa, M.; Yoshida, W.; Kurita, S.; Takada, S.; Yoshii, F. *Macromolecules* **1997**, *30*, 1782−1786.
(49) Snively, C. M.; Koenig, J. L. *Macromolecules* **1998**, *31*, 3753−3755.
(50) Buback, M.; Kowollik, C. *Macromolecules* **1998**, *31*, 3211−3215.
(51) Ozaki, Y.; Liu, Y.; Noda, I. *Macromolecules* **1997**, *30*, 2391−2399.
(52) Ren, Y.; Murakami, T.; Nishioka, T.; Nakashima, K.; Noda, I.; Ozaki, Y. *Macromolecules* **1999**, *32*, 6307−6318.
(53) Rigler, P.; Ulrich, W.-P.; Hoffmann, P.; Mayer, M.; Vogel, H. *ChemPhysChem* **2003**, *4*, 268−275.
(54) Moller, K. C.; Santner, H. J.; Kern, W.; Yamaguchi, S.; Besenhard, J. O.; Winter, M. *J. Power Sources* **2003**, *119−121*, 561−566.
(55) Morvan, J.; Camelot, M.; Zecchini, P.; Roques-Carmes, C. *J. Colloid Interface Sci.* **1984**, *97*, 149−156.
(56) Clerk, P.; Simon, S. *Strukturaufklärung Organischer Verbindungen*, 3rd ed.; Springer-Verlag: Berlin, 1986.
(57) Smith, A. L. *Spectrochim. Acta* **1960**, *16*, 87−105.
(58) Launer, P. J. In *Silicon Compounds, Register and Review*, 4th ed.; Arkles, B., Ed.; Petrarch Systems: Bristol, PA, 1987; p 100.
(59) Lucovsky, G.; Wong, C. K.; Pollard, W. B. *J. Non-Cryst. Solids* **1983**, *59−60*, 839−846.
(60) Pai, P. G.; Chao, S. S.; Takagi, Y.; Lucovsky, G. *J. Vac. Sci. Technol., A* **1986**, *4*, 689−694.
(61) Vasant, E. F.; Van der Voort, P.; Vrancken, K. C. *Studies in Surface Science and Catalyis: Vol. 93, Characterization and Chemical Modification of the Silica Surface*; Elsevier Science: Amsterdam, 1995.
(62) Morvan, J.; Camelot, M.; Zecchini, P.; Roques-Carmes, C. *J. Colloid Interface Sci.* **1984**, *97*, 149−156.
(63) Balykova, T. N.; Rode, V. V. *Usp. Khim.* **1969**, *38*, 662−686.
(64) Lee, L.-H. *J. Adhes.* **1972**, *4*, 39−49.
(65) Mirzadeh, H.; Khorasani, M.; Sammes, P. *Iran. Polym. J.* **1998**, *7*, 5−13.
(66) Kim, H.; Urban, M. W. *Langmuir* **1996**, *12*, 1047−1050.
(67) Kim, H.; Urban, M. W. *Langmuir* **1999**, *15*, 3499−3505.
(68) Hollahan, J. R.; Carlson, G. L. *J. Appl. Polym. Sci.* **1970**, *14*, 2499−2508.
(69) Gaboury, S. R.; Urban, M. W. *Adv. Chem. Ser.* **1993**, *236*, 777−790.
(70) Baulch, D. L.; Cox, R. A.; Crutzen, P. J.; Hampson, R. F., Jr.; Kerr, J. A.; Troe, J.; Watson, R. T. *J. Phys. Chem. Ref. Data* **1982**, *11*, 327−496.
(71) Eliasson, B.; Kogelschatz, U. *Ozone: Sci. Eng.* **1991**, *13*, 365−373.
(72) Burkus, F. S., II; Amarasekera, J. *Rubber World* **2000**, *222*, 26−35.
(73) Cefalas, A. C.; Sarantopoulou, E.; Gogolides, E.; Argitis, P. *Microelectron. Eng.* **2000**, *53*, 123−126.

MA049747Q